Acta metall. Vol. 34, No. 12, pp. 2493–2499, 1986
Printed in Great Britain.

0001-6160/86 $3.00 + 0.00

OBSERVATION OF AN ADIABATIC SHEAR BAND IN TITANIUM BY HIGH-VOLTAGE TRANSMISSION ELECTRON MICROSCOPY

M. A. MEYERS† and HAN-RYONG PAK

Center for Explosives Technology Research and Department of Metallurgical and Materials Engineering, New Mexico Institute of Mining and Technology, Socorro, NM 87801, U.S.A.

(*Received* 27 *July* 1984; *in revised form* 28 *October* 1985)

Abstract—An adiabatic shear band produced by the impact of a cylindrical projectile on a target of commercial purity titanium was observed by high-voltage transmission electron microscopy. While the material in the vicinity of the shear band showed a high density of dislocations and deformation twins, the structure of the shear band consisted of small (0.05–0.3 μm) grains with well defined high-angle grain boundaries. The boundary between the matrix and the shear-band material is very well defined showing that the localized deformation regime within the band requires a temperature–strain threshold to become operative. Calculations suggest that the microcrystalline structure is formed during the shear band propagation stage. A simple model for plastic deformation in the shear band is proposed.

Résumé—Nous avons observé par microscopie électronique à haute tension une bande de cisaillement adiabatique produite par l'impact d'un projectile cylindrique sur une cible de titane de pureté commerciale. Alors que le matériau présentait au voisinage de la bande de cisaillement une forte densité de dislocations et de macles méchaniques, la structure de la bande de cisaillement consistait en de petits grains (0,05–0,3 μm) avec des joints de grains de forte désorientation bien définis. La limite entre la matrice et la bande de cisaillement est très bien définie, ce qui montre que le régime de déformation localisée dans la bande nécessite un seuil de température–déformation pur devenir opérationnel. Les calculs donnent à penser que la structure microcristalline se forme au cours du stade de propagation de la band de cisaillement. Nous proposons un modèle simple pour la déformation plastique dans le bande de cisaillement.

Zusammenfassung—Ein adiabatisches Scherband, welches durch Aufprall eines zylindrischen Geschosses auf ein Ziel aus kommerziell reinem Titan erzeugt worden war, wurde in einem Hochspannungsdurchstrahlungselektronenmikroskop untersucht. In der Nähe des Scherbandes fand sich eine hohe Dichte an Versetzungen und Verformungszwillingen; die Struktur des Scherbandes dagegen bestand in kleinen Körnern (0,05–0,3 μm) mit wohl definierten Großwinkelkorngrenzen. Die Grenze zwischen Matrix und Scherbandbereich ist sehr gut definiert; dieser Befund zeigt, daß die lokalisierte Verformung innerhalb des Bandes eine Temperatur/Dehnungsschwelle überwinden, muß, bevor sie einsetzt. Rechnungen legen nahe, daß die mikrokristalline Struktur sich während der Ausbreitung des Scherbandes ausbildet. Für die plastische Verformung im Scherband wird ein einfaches Modell vorgeschlagen.

1. INTRODUCTION

The adiabatic shear band is an important mode of deformation at high strain rates. In ballistic deformation, it has been clearly identified, in many alloy systems, as the precursor to fracture and fragmentation. Olson *et al.* [1] defined it as a strain localization phenomenon generally attributed to a plastic instability arising from thermal softening during adiabatic or quasi-adiabatic deformation. While a considerable amount of effort has been devoted to understanding the microstructural effects and to modelling the thermomechanical environment required for the formation of these instabilities, detailed analysis by transmission electron microscopy has only been carried out in a few alloy systems. To the authors' knowledge, transmission electron microscopy has been conducted by the following investigators: Craig and Stock [2] (70-30 brass), Stock and Thompson [3] (aluminium alloy 2014), Glenn and Leslie [4] (alloy steel in quenched and tempered condition), Wingrove [5] (alloy steel in quenched and tempered condition), Me-Bar and Shechtman [6] (Ti–6A1–4V alloy) and Mataya *et al.* [7] (precipitation strengthened austenitic stainless steel). Ringlike diffraction patterns were observed in these studies, but the microstructural features could not be clearly identified.

2. EXPERIMENTAL

The alloy used in this study was commercial purity titanium (0.02% C, 0.04% Fe, 0.012% N, 0.12% O) annealed at 800°C for 1 h. The grain size, measured by the linear intercept technique, was 61 μm. The titanium plate, with a thickness of 12.5 mm, was impacted at a velocity of 600 m/s by a cylindrical steel projectile having a diameter of 3 mm. The penetration into the target was approximately 6 mm. The

†Currently at U.S. Army Research Office, Research Triangle Park, NC 27709, U.S.A.

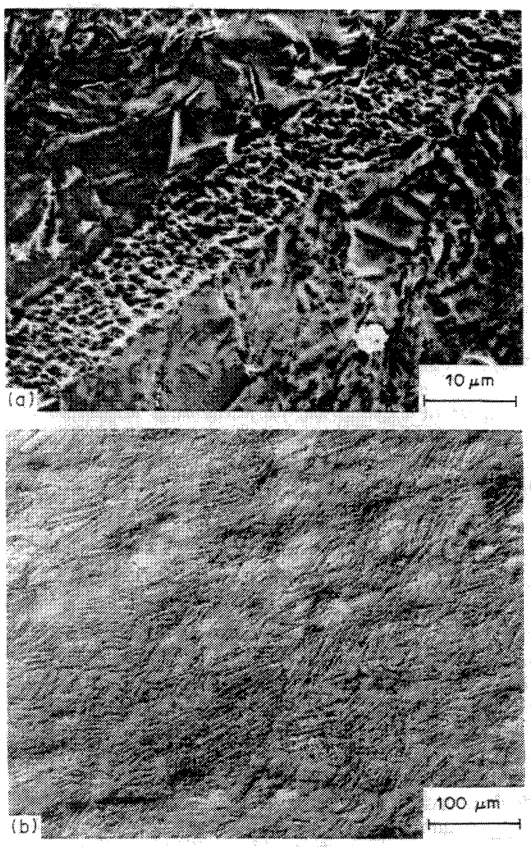

Fig. 1. (a) Scanning electron micrograph of shear band in commercial purity titanium. (b) Optical micrograph of homogeneous deformation region in proximity of projectile; deformation twins can be seen in most grains.

experimental procedure is described in greater detail by Grebe *et al.* [8].

For transmission electron microscopy, 3 mm disks containing a shear band passing through the center were prepared and thinned in a Fishione jet electropolisher. One side of the disk was coated with "stop off", exposing only the band area, in order to ensure preferential thinning of the shear band. A KRATOS EM-1500 transmission electron microscope, operating at 1.5 MeV, was used through the courtesy of the National Center for Electron Microscopy, Lawrence Berkeley Laboratory, California.

3. OBSERVATIONS

Figure 1(a) shows a micrograph of the adiabatic shear band. Approximately 15 bands were observed on the section of the target made along the axis of the projectile. The band widths varied between 1 and 10 μm and the grains were sectioned by the bands. These bands are similar to the ones observed by Winter [9], Winter and Hutchings [10], and Timothy and Hutchings [11] in titanium. No clear microstructural features can be detected optically. Regions away from the shear bands, but close to the impact surface [Fig. 1(b)], show profuse twinning, in accordance with results obtained by Koul and Breedis [12].

Figure 2 shows a high-voltage transmission electron micrograph of the shear band and the adjoining matrix. The arrows show the boundaries between the shear band and the matrix. Very small grains and well defined grain boundaries (seen more readily in Figs 3 and 4) can be observed within the shear band, which presents a fairly uniform microstructure. The matrix shows the high density of dislocations. The selected area diffraction patterns of the matrix (M) and shear band (SB) evidence the contrasting features. While the former shows the h.c.p. reflections ([1$\bar{1}$01] zone) from one crystal, the latter shows reflections of multiple grains, forming discontinuous h.c.p. rings. The structure of the individual micrograins is crystalline. The micrograin morphology does not change significantly from the center of the band towards the matrix, indicating that the material did not melt. Solidification would most probably produce colum-

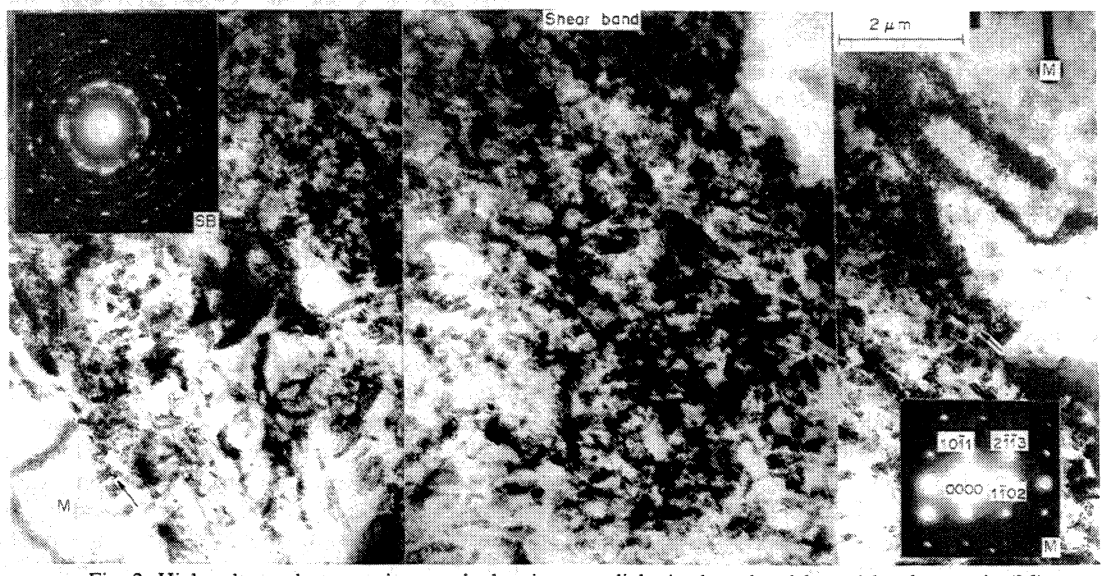

Fig. 2. High-voltage electron micrograph showing an adiabatic shear band bound by the matrix (M).

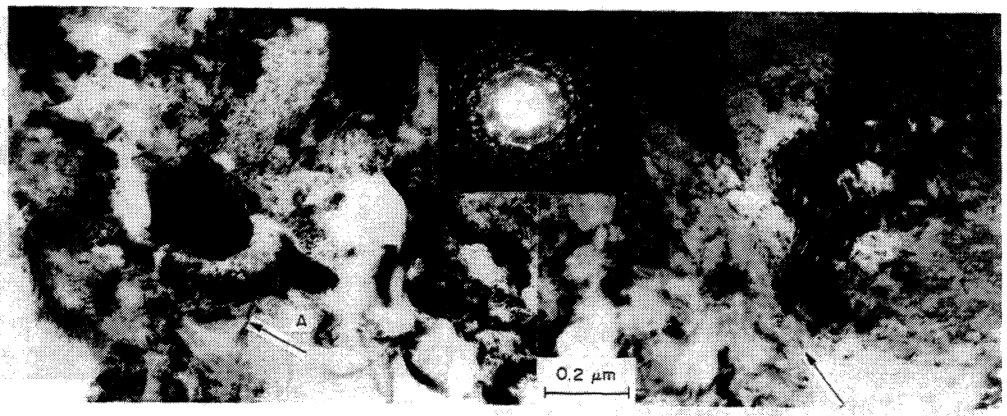

Fig. 3. A closer view of the adiabatic shear band, showing Moiré fringe patterns produced at a boundary between micrograins. Arrow A indicates interfacial dislocations.

nar grains in the vicinity of the shear band–matrix interface. Figure 3 shows a closer view of the micrograins. Moiré fringes (marked by arrow A) show a rather regular pattern and the dislocation density in the grain boundary is not high. Similar structures are seen in other areas of the figure. The grains are equiaxed. The grain shape is better defined in Fig. 4, which is a dark-field micrograph made through one of the strong $1\bar{1}00$ reflections. The micrograins vary in size from 0.05 to 0.3 μm. The dislocation density in the grains is in general not very high; it seems to be somewhat higher in the larger grains as can be seen in Figs 3 and 4. Figure 5 shows in greater detail parallel and regularly spaced Moiré fringe patterns indicating that no dislocations exist in the small grains.

4. ANALYSIS

For the purpose of rendering the behavior of titanium under study more clearly understood, an "adiabatic" stress–strain curve was developed. Figure 6 shows the shear stress–shear strain curves; the isothermal curves are ideally represented as straight lines and were obtained by interpolation from experimental low strain-rate tests conducted by Conrad *et al.* [13]. This interpolation was made by assuming a linear stress–strain response at all temperatures for the tests conducted by Conrad *et al.* [13]. Low strain-rate data were used because of unavailability of high strain-rate data. For comparison purposes, Wulf [14] performed tests on commercial purity titanium at ambient temperature and obtained flow

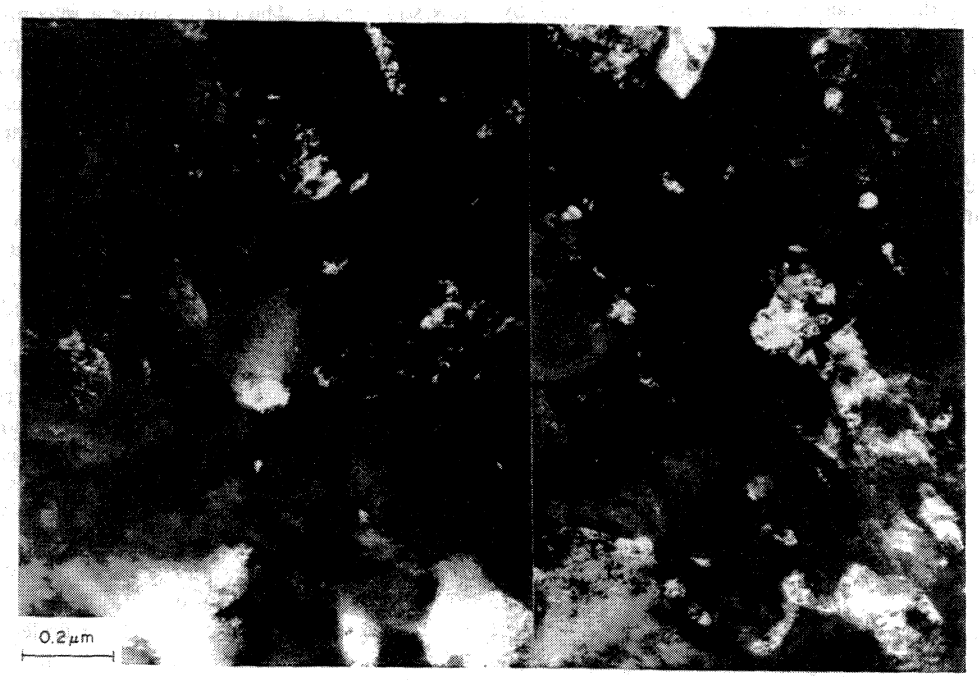

Fig. 4. Dark field electron micrograph of the shear band taken by $10\bar{1}0$ reflection, showing the shape of micrograins in the band. The grain size ranges from 0.05 to 0.3 μm.

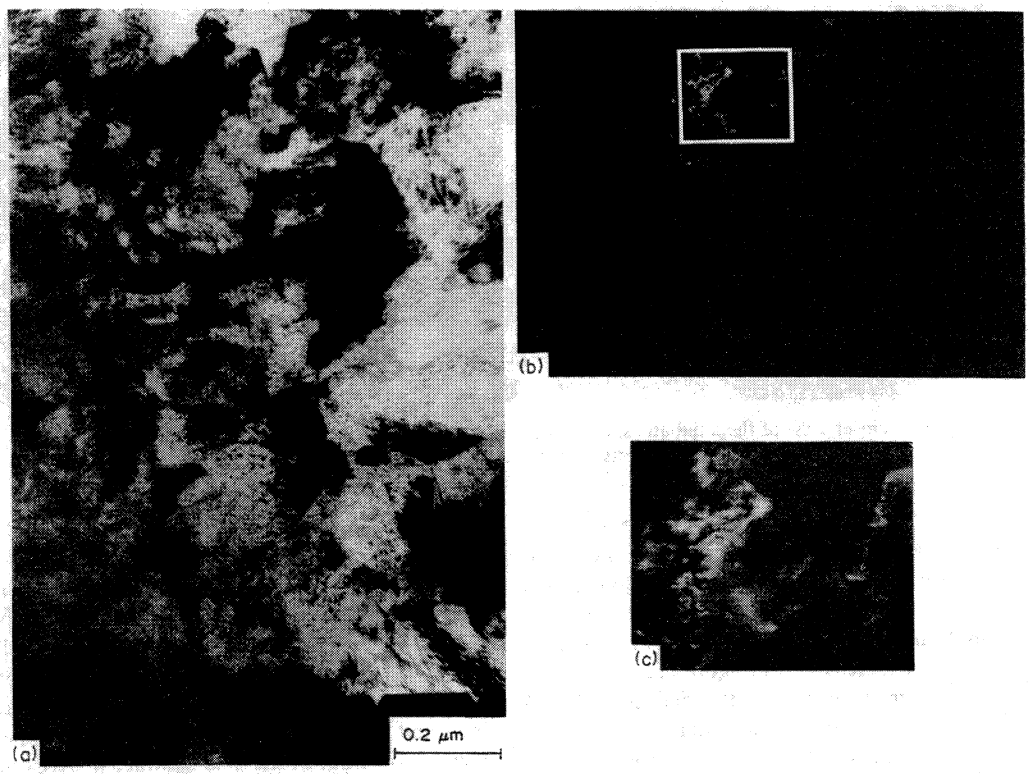

Fig. 5. Electron micrographs of the shear band, showing parallel and regularly spaced Moire' fringe patterns produced at a boundary between very small grains. (a) Bright field; (b) dark field; (c) dark field of the framed region in (b).

stresses (at a nominal strain of 0.1) between 550 and 700 MPa at strain rates between 2×10^3 and $2 \times 10^4\ s^{-1}$, respectively. This corresponds to shear stresses in the 275–350 MPa range. Hence, the difference is not drastic. The adiabatic curve (which intersects the isothermal curves) was obtained by assuming that all of the work of deformation is converted into heat. The computations were done numerically, with shear strain increments of 0.1. For each increment the area of the stress strain curve was computed; this energy was converted into temperature increase by using the (temperature-dependent) heat capacity. The increase in temperature was then converted into a decrease of stress by linear interpolation between the two closest values shown by the straight isothermal lines (at 100°C intervals). This adiabatic curve clearly shows that the material response is vastly different at high strain rates from low strain rates. The curve shows a maximum at a shear strain of 1; beyond that value, thermal softening dominates work hardening. This is the domain in which the adiabatic shear band becomes stable. This instability strain corresponds to a temperature of approx. 350°C. It can be seen that the rate of "softening" decreases at higher strains by virtue of less deformation energy generated at the higher temperatures. In spite of the simplifying assumptions in Fig. 6 it is clear that instability sets in at $\gamma = 1$. This value is surprisingly close to earlier predictions. Recht [16] predicted an instability shear strain of 0.64 according to Culver's [15] calculations; Culver [16] performed torsional impact experiments on titanium and obtained $1.00 < \gamma_i < 1.25$. His calculations predict $\gamma_i = 1.2$–1.4. The shear strain within a shear band has been found to reach, in some materials, values exceeding 500. For a Ti–6% Al–4 % V alloy impacted under conditions similar to the titanium studied in this investigation, shear strains of 5 were found. Hence, the temperature within the shear band could have reached 800°C. Titanium undergoes the h.c.p.→b.c.c. transformation at 883°C and melts at 1669°C. Melting is not likely to have occurred in the shear band; the absence of b.c.c. reflections in

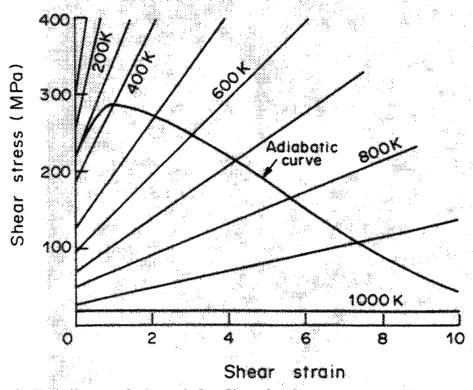

Fig. 6. Isothermal (straight lines) shear stress–shear strain response of commercial purity titanium between 100 and 1000 K; adiabatic shear stress–shear strain curve showing maximum at $\gamma = 1.2$.

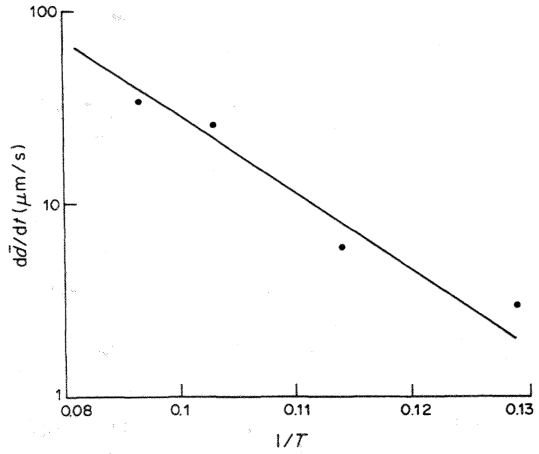

Fig. 7. Rate of increase of grain diameter ($d\bar{d}/dt$) vs inverse of temperature for Battelle titanium (0.2 at.% O_{eq}). Data extracted from Fig. 3 of Okazaki and Conrad [17].

the shear-band area also is indicative that the h.c.p.→b.c.c. transformation did not occur.

If one then assumes that the temperature within the shear band reached 800°C during deformation, it is logical to inquire whether the microcrystalline and virtually dislocation-free structure was formed during the deformation stage or after deformation, during cooling. Indeed, Winter [9] suggested that the microstructure of the band was formed during the cooling stage. The recrystallization behavior of titanium was studied by Okazaki and Conrad [17]. In order to predict the recrystallization rate in the present case, the initial grain-growth rates of Battelle titanium (0.2 at.% Oe) were taken as the tangents of the grain diameter vs time curves at time zero. The justification for this comes from the fact that, at the initial stages of the grain-growth curves, one actually has recrystallization. The plots of Okazaki and Conrad [17] clearly indicate a rapid decrease in the grain-growth rate with time. Their observations by TEM show that recrystallization was not complete. These growth rates are shown in the Arrhenius plot of Fig. 7. Assuming a singly activated process, the recrystallization response of the material can be represented by the equation.

$$\frac{d\bar{d}}{dt} = 4.3\, e^{-38.7/T} \tag{1}$$

where $\bar{d}$ is the mean recrystallized grain size. In order to determine whether the recrystallized grains observed in Figs 2–5 were produced during the band formation (or propagation) stage or during the cooling stage, an approximate calculation of the cooling rate of the band was performed. This calculation used the finite difference method and a semi-infinite slab. Heat was deposited on the free surface of the slab at a rate such that the temperature was constant and equal to 1073 K. The temperatures at distances of 2 and 4.5 μm of the band center were calculated. The observations and calculations indicate that the temperature in the band could have reached 800°C. This value was used for the heat dump at the surface. When the temperature at the edge of the shear band (assumed to have a thickness of 9 μm) reached the value of 700°C, the heat input was stopped. Figure 8 shows very clearly the temperatures as a function of time, at three positions: surface (center of band), 2 μm from band center, and 4.5 μm from band center (band edge). The temperature at the center is maintained constant until shut-off, which occurs when the temperature of the edge reaches 700°C. This takes place at a time equal to 10^{-5} s. The cooling rates at the center and edge of the band are not too different

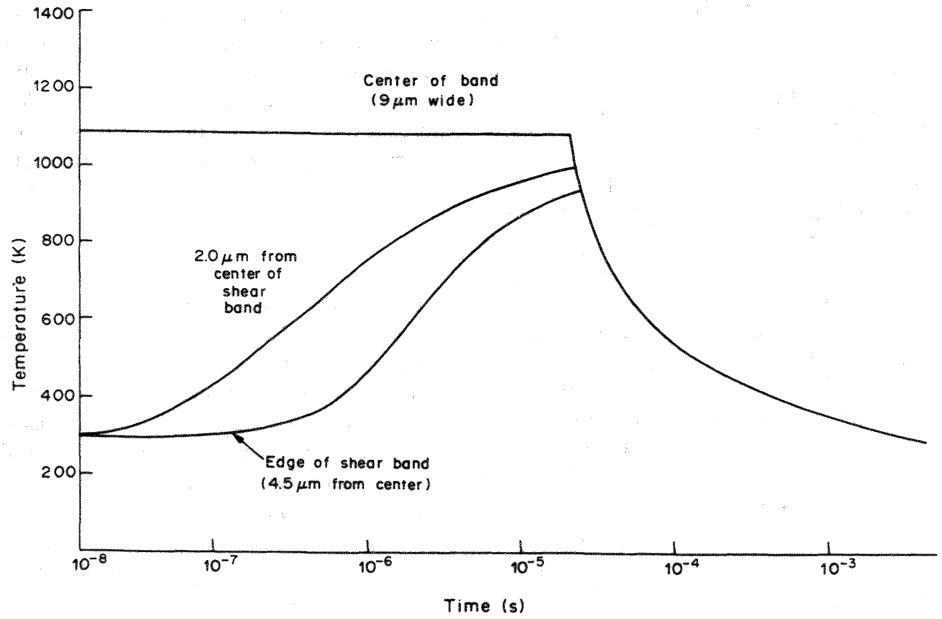

Fig. 8. Rate of cooling of shear band after deformation predicted from heat transfer calculations assuming a constant temperature of 1073 K at center of band as band is being formed.

from that point on, and the temperature reaches ambient temperature at 3×10^{-3} s. The finite difference computation can be verified by Carslaw and Jaeger [18]. They present the derivation and prediction of temperature for an infinite solid in which an internal region of thickness $2a$ is set initially at a temperature T_i, the surroundings being at zero. At time $t = 0$, $T = T_i$ for $-a < x < a$ and $T = 0$ in the surroundings. Figure 4(a) of Carslaw and Jaeger [18] presents the normalized temperatures T/T_i as a function of x/a for different values of kt/a^2, where k is the thermal diffusivity. Using a constant heat capacity of $455\,\mathrm{Jkg^{-1}K^{-1}}$ and heat conductivity of $0.2\,\mathrm{Js^{-1}cm^{-1}}$, one finds that $T/T_i = 0.5$ inside the band is reached at $t = 2.5\,\mu$s. This value is as expected, shorter than the predictions from the calculation represented in Fig. 8. While Carslaw and Jaeger's [18] computation assumes heat transfer starting at time $t = 0$ with full band formed instantaneously, finite difference computation assumes transfer to surrounding while band is being formed (thickness increasing). Thus, cooling rate is much lower in the more realistic finite-difference computation. The cooling in Fig. 8 is fairly well represented by

$$T = 0.162t^{-0.791} + 298 \tag{2}$$

where T is the temperature in Kelvin and t is the time in seconds. But substituting equation (2) for equation (1) and integrating one obtains

$$\bar{d}_f - \bar{d}_0 = 4.3 \int_{t_1}^{t_2} \exp \frac{-38.7}{0.162\,t^{-0.791} + 298}\,\mathrm{d}t \tag{3}$$

$\bar{d}_0$, the initial grain size can be set as zero (nucleus for recrystallization). The integration limits are taken from Fig. 8 and are the times corresponding to the temperatures of 1073 and 298 K. Definite integration was carried out and the final grain size, $\bar{d}_f$, was found to be equal to $3.8 \times 10^{-3}\,\mu$m. This value is lower, by one to two orders of magnitude, than the observed recrystallized micrograins (0.05–0.3 μm). Thus, one can conclude that the structure observed in Figs 2–5 was not produced during cooling, but results from the propagation stage.

A micromechanical mechanism for the propagation of shear bands has been proposed by Coffey and Armstrong [19] and Armstrong *et al.* [20]. It is based on the catastrophic release of a dislocation pile-up, causing localized heating on the slip plane. This model is specifically directed at explosives, which are known to detonate by hot spots. The shear band/pile-up release theory is an alternative to the pore collapse theory in explaining initiation and propagation of a detonation front. Winter and Field [21] also studied the initiation of explosives and found that localized plastic flow (shear localization) played a key role. However, the microstructural observations reported in Section 3 do not provide any direct evidence for the dislocation avalanche concept. The process leading to the formation of the micrograins seems to be dynamic recrystallization. Although any

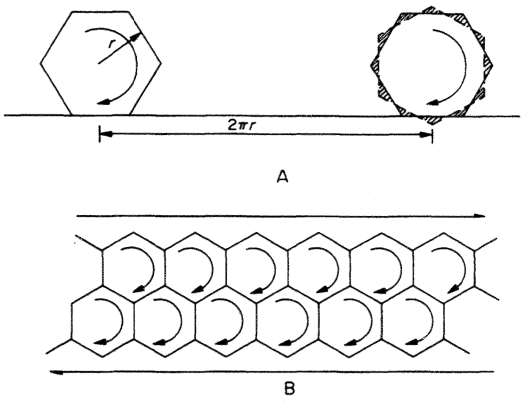

Fig. 9. Proposed mechanism for shear band propagation involving micrograin rotation and sliding of micrograin boundaries. (a) Micrograin rotating by 2π and translating by $2\pi r$ in process; hatching indicates regions in which substantial plastic deformation has to take place. (b) Array of rotating micrograins producing translation of upper part of band with respect to lower part.

proposed mechanism for the formation and propagation of the shear bands is speculatory at this point, a few thoughts can be advanced. The adiabaticity (or quasi-adiabaticity) of the process is responsible for the temperature rise and thermal softening within the bands. As plastic deformation intensifies itself (strains of 500 have been reported in shear bands [22]), the band region undergoes dynamic recrystallization. This leads to the grain size reduction. An equilibrium temperature is achieved at which deformation takes place primarily by micrograin boundary sliding. This is a mechanism favored at high temperatures, and creep and superplasticity take place primarily by grain-boundary sliding. The geometrical constraints inside a shear band are such that sliding produces rotation of the micrograins. The right-hand side of Fig. 9(a) shows two positions of the micrograin, schematically represented by a hexagon. Hatching indicates the regions which will experience substantial plastic deformation due to strain incompatibility between adjacent grains. The central portion of the grains, on the other hand, does not undergo significant plastic deformation. A 360° rotation of one grain will generate a shear strain

$$\gamma = \frac{2\pi r}{2r} = \pi. \tag{4}$$

Figure 9(b) shows the rotation of successive layers of micrograins leading to shear in the band. A very simple model of this deformation mechanism can be made by taking a pencil (cylinder) and rolling it between the two hands. The mechanism proposed here is conceptually similar to Ashby and Verrall's [23] mechanism for superplasticity (except that diffusion accommodates the strains in the latter). The deformation takes place without deforming the grains to the same extent as the total strain. Ashby and Verrall [23] apply their mechanism to tensile and compressive stresses and they only have micrograin translation. Inside a shear band, and due to the

geometrical constraints, rotation is needed if the band width is constant. In the shear band, the plastic strain accommodation required in rotation [shown by the hatched areas in Fig. 9(a)] does not take place by diffusion, but by dislocation generation and motion. This process takes place at high temperatures, so that these dislocations are annealed out. The application of the concept of superplasticity in shear-band propagation is not an original thought of the present authors, but has been discussed previously by Hatherly and Malin [24], for shear bands produced by rolling. Hatherly and Malin [24] also point out that superplasticity (in the shear band) would have to occur at strain rates 100–1000 times higher than those involved in classical superplasticity. Hatherly and Malin's [24] remarks apply to 70:30 brass. The microstructure observed in the present work, and evidence (from calculations) that they are produced during (and not after) deformation, indicate that some type of grain-boundary sliding mechanism might be operational, leading to micrograin rotation.

Acknowledgements—The use of the KRATOS EM-1500 at the National Center of Electron Microscopy, Lawrence Berkeley Laboratory, was made possible by a special Department of Energy arrangement. Professor K. Westmacott and Mr D. Ackland should be acknowledged in this regard. The help of Mr H. A. Grebe in specimen preparation is greatly appreciated. Mr S. N. Chang and Mr C. Wittman provided valuable help by performing the calculations. This research was supported by National Science Foundation Grant DMR 8115127 and by the Center for Explosives Technology Research. Dr P.-A. Persson's assistance by performing the Carslaw and Jaeger calculation is greatly appreciated.

REFERENCES

1. G. B. Olson, J. F. Mescall and M. Azrin, in *Shock Waves and High-Strain-Rate Phenomena in Metals: Concepts and Applications* (edited by M. A. Meyers and L. E. Murr), p. 221. Plenum Press, New York (1981).
2. T. A. C. Stock and K. R. L. Thompson, *Metall. Trans.* **1,** 219 (1970).
3. J. V. Craig and T. A. C. Stock, *J. Aust. Inst. Metals* **15,** 1 (1970).
4. R. C. Glenn and W. C. Leslie, *Metall. Trans.* **2,** 2945 (1971).
5. A. L. Wingrove, *J. Aust. Inst. Metals* **16,** 67 (1971).
6. Y. Me-Bar and D. Shechtman, *Mater. Sci. Engng* **58,** 181 (1983).
7. M. C. Mataya, M. J. Carr and G. Krauss, *Metall. Trans.* **13A,** 1263 (1982).
8. H. A. Grebe, H-r. Pak and M. A. Meyers, *Metall. Trans.* **16A,** 761 (1985).
9. R. E. Winter, *Phil. Mag.* **31,** 765 (1975).
10. R. E. Winter and I. M. Hutchings, *Wear* **34,** 141 (1975).
11. S. P. Timothy and I. M. Hutchings, in *High Energy Rate Fabrication—1984* (edited by I. Berman and J. W. Schroeder), p. 31. Am. Soc. Mech. Engrs, New York (1984).
12. M. K. Koul and J. F. Breedis, in *The Science, Technology, and Application of Titanium* (edited by R. I. Jaffee and N. E. Promisel), p. 817. Pergamon Press, New York (1968).
13. H. Conrad, M. Doner and B. DeMeester, in *Titanium Science and Technology*, p. 969. Plenum Press, New York (1973).
14. G. L. Wulf, *Int. J. Mech. Sci.* **21,** 719 (1979).
15. R. S. Culver in *Metallurgical Effects at High Strain Rates* (edited by R. W. Rohde, B. M. Butcher, J. R. Holland and C. H. Karnes), p. 519. Plenum Press, New York (1973).
16. R. F. Recht, *J. appl. Mech.* **31,** 189 (1974).
17. K. Okazaki and H. Conrad, *Metall. Trans.* **3A,** 2411 (1972).
18. H. S. Carslaw and J. C. Jaeger, *Conduction of Heat in Solids*, 2nd edn, pp. 54–57. Oxford (1959).
19. C. S. Coffey and R. W. Armstrong, source cited in Ref. [1], p. 313.
20. R. W. Armstrong, C. S. Coffey and W. L. Elban, *Acta metall.* **30,** 2111 (1982).
21. R. E. Winter and J. E. Field, *Proc. R. Soc., Lond.* **343A,** 399 (1975).
22. G. L. Moss, source cited in Ref. [1], p. 299.
23. M. F. Ashby and R. A. Verrall, *Acta metall.* **21,** 149 (1973).
24. M. Hatherly and A. S. Malin, *Scripta metall.* **18,** 449 (1984).